

Finite Element Modelling of TRIP Steels

Ioannis Papatriantafillou, Nikolaos Aravas and Gregory N. Haidemenopoulos

Department of Mechanical and Industrial Engineering, University of Thessaly, Volos / Greece

A constitutive model that describes the mechanical behaviour of steels exhibiting "Transformation Induced Plasticity" (TRIP) during martensitic transformation is presented. Multiphase TRIP steels are considered as composite materials with a ferritic matrix containing bainite and retained austenite, which gradually transforms into martensite. The effective properties and overall behaviour of TRIP steels are determined by using homogenization techniques for non-linear composites. The developed constitutive model considers the different hardening behaviour of the individual phases and estimates the apportionment of plastic strain and stress between the individual phases of the composite. A methodology for the numerical integration of the resulting elastoplastic constitutive equations in the context of the finite element method is developed and the constitutive model is implemented in a general-purpose finite element program. The prediction of the model in uniaxial tension agrees well with the experimental data. The problem of necking of a bar in uniaxial tension is studied in detail.

Keywords: TRIP steels, TRIP plasticity, strain-induced martensitic transformation, finite element modelling.

Introduction

TRIP-aided multiphase steels are a new generation of low-alloy steels that exhibit an enhanced combination of strength and ductility satisfying the requirements of automotive industry for good formable high-strength steels. After thermal treatment TRIP steels obtain a triple-phase microstructure consisting of ferrite, bainite and retained austenite. Retained austenite is metastable at room temperature and transforms to martensite during straining. TRIP steels are essentially composite materials with evolving volume fractions of the individual phases. A constitutive model for TRIP steels is developed in this paper. The total strain is assumed to be the sum of elastic, plastic and transformation parts. The plastic part is determined by using homogenization techniques for non-linear composites that have been developed recently by Ponte-Castañeda, Suquet and co-workers [7, 9, 10]. The transformation strain rate has both deviatoric and volumetric parts and is proportional to the rate of change of the volume fraction of martensite. The evolution of martensite due to martensitic transformation is described by a kinetic model which takes into account temperature, plastic strain and stress state. The model proposed considers the different hardening behaviour of the individual phases and estimates the different levels of strain accumulated by the constituent phases. A methodology for the numerical integration of the resulting non-linear constitutive equations is developed and implemented in a general-purpose finite element program (ABAQUS). Experimental data from interrupted tensile tests in specific TRIP steel are used for the calibration of the constitutive model. The calibrated model is used together with the finite element method for the analysis of necking in uniaxial tension.

Constitutive modelling

Multiphase TRIP steels are considered as four-phase composite materials with a ferritic matrix containing bai-

nite, austenite and martensite. The following labels are used for the individual phases: (1)=martensite, (2)=austenite, (3)=bainite and (4)=ferrite. The corresponding volume fractions of the phases are $c^{(r)}$, $r = 1, 2, 3, 4$, where

$$\sum_{r=1}^4 c^{(r)} = 1.$$

The rate of deformation tensor \mathbf{D} is decomposed into elastic, plastic and transformation parts:

$$\mathbf{D} = \mathbf{D}^e + \mathbf{D}^p + \mathbf{D}^{TRIP}. \quad (1)$$

Elastic behaviour. The elastic properties of the individual phases are almost identical. Therefore, TRIP steels can be considered as homogenous in the elastic region. A hypoelastic equation of the form

$$\mathbf{D}^e = \mathbf{M}^e : \overset{\nabla}{\boldsymbol{\sigma}} \quad \overset{\nabla}{\boldsymbol{\sigma}} = \mathbf{L}^e : \mathbf{D}^e \quad (2)$$

is used, where \mathbf{M}^e is the isotropic elastic compliance tensor, $\mathbf{L}^e = \mathbf{M}^{e-1}$ is the elastic stiffness tensor and $\overset{\nabla}{\boldsymbol{\sigma}}$ is the Jaumann derivative of the Cauchy (true) stress tensor.

Transformation deformation rate. A critical aspect of the transformation process is the strain softening which occurs as a result of the transformation strain. This is incorporated into the model by introducing the deformation rate \mathbf{D}^{TRIP} , which is proportional to the rate of the martensite volume fraction $\dot{f} = \dot{c}^{(1)}$. The transformation deformation rate consists of a deviatoric term that models the transformation shape strain and of a dilatational term accounting for the positive transformation volume change (Stringfellow et al. [8]):

$$\mathbf{D}^{TRIP} = A (\sigma_{eq}) \dot{f} \mathbf{N} + \frac{\dot{\varepsilon}_v^p}{3} \boldsymbol{\delta}, \quad \mathbf{N} = \frac{3}{2} \frac{\mathbf{s}}{\sigma_{eq}} \quad (3)$$

where \mathbf{s} is the deviatoric stress tensor, $\sigma_{eq} = \sqrt{3 s_{ij} s_{ij}/2}$ is the von Mises equivalent stress, $\boldsymbol{\delta}$ is the second-order identity tensor and $\dot{\epsilon}_v^p = D_{kk}^{TRIP}$ is the transformation dilatation rate, the value of which is defined later in this section. The dimensionless coefficient A reflects an ensemble effect of the shape strains over an isotropic orientational distribution of nucleation sites as considered by Olson, Tzusaki and Cohen [5] and, according to experimental data, is taken to depend on the equivalent stress as follows:

$$A(\sigma_{eq}) = A_0 + A_1 \frac{\sigma_{eq}}{s_a^*} \quad (4)$$

where A_0 and A_1 are constants and s_a^* is a reference austenite stress.

The dilatation rate $\dot{\epsilon}_v^p = D_{kk}^{TRIP}$ is determined by taking into account that the volume change associated with the martensitic transformation can be written in the form

$$dV^m = -(1 + \Delta_v) dV^a \quad (5)$$

where dV^m and dV^a are the volume changes of martensite and austenite respectively, and Δ_v is the relative volume change and takes values in the range 0.02 to 0.05 (Stringfellow et al. [8]). Since changes in volume due to elastic strains are small and fully recoverable, it is assumed that changes in dilatation are due to volumetric plastic deformation rates only. Thus, taking into account that $\dot{\epsilon}_v^p = \dot{V}/V$, and using (5), we can show readily that

$$\frac{\dot{V}^m}{V} = \frac{1 + \Delta_v}{\Delta_v} \dot{\epsilon}_v^p \quad \text{and} \quad \frac{\dot{V}^a}{V} = -\frac{\dot{\epsilon}_v^p}{\Delta_v}$$

where V is the total volume. Then, using the definitions $f \equiv c^{(1)} = V^m/V$ and $c^{(a)} \equiv c^{(2)} = V^a/V$, we can show that

$$\begin{aligned} \dot{f} &= \frac{1 + (1 - f) \Delta_v}{\Delta_v} \dot{\epsilon}_v^p \quad \text{or} \\ \dot{\epsilon}_v^p &= \frac{\Delta_v}{1 + (1 - f) \Delta_v} \dot{f} \cong \Delta_v \dot{f} \quad \text{and} \\ \dot{c}^{(a)} &= -\left(\frac{1}{\Delta_v} + c^{(a)}\right) \dot{\epsilon}_v^p \\ &= -\left(\frac{1}{\Delta_v} + c^{(a)}\right) \frac{\Delta_v}{1 + (1 - f) \Delta_v} \dot{f} \cong \\ &\cong -[1 - (1 - f - c^{(a)}) \Delta_v] \dot{f}. \end{aligned}$$

Taking into account that $f + c^{(a)} + c^{(3)} + c^{(4)} = 1$, we can write the last equation as

$$\dot{c}^{(a)} \cong -[1 - (c^{(3)} + c^{(4)}) \Delta_v] \dot{f}.$$

Similarly, using the definitions $c^{(3)} = V^{(3)}/V$ and $c^{(4)} = V^{(4)}/V$, we conclude that

$$\dot{c}^{(3)} = -c^{(3)} \dot{\epsilon}_v^p \cong -c^{(3)} \Delta_v \dot{f}$$

and

$$\dot{c}^{(4)} = -c^{(4)} \dot{\epsilon}_v^p \cong -c^{(4)} \Delta_v \dot{f}.$$

Finally, substituting the expression $\dot{\epsilon}_v^p \cong \Delta_v \dot{f}$ in (3), we conclude that the constitutive equation for \mathbf{D}^{TRIP} can be written as

$$\mathbf{D}^{TRIP} = \left[A(\sigma_{eq}) \mathbf{N} + \frac{\Delta_v}{3} \boldsymbol{\delta} \right] \dot{f}. \quad (6)$$

The plastic part of the deformation rate. The effective plastic deformation rate is determined using a viscoplastic constitutive equation of the form:

$$\mathbf{D}^p = \frac{1}{2} \theta^{\text{hom}} \mathbf{s} = \dot{\epsilon}^p \mathbf{N}, \quad \dot{\epsilon}^p = \frac{1}{3} \sigma_{eq} \theta^{\text{hom}} \quad (7)$$

where θ^{hom} is the effective viscous compliance that depends on the macroscopic von Mises equivalent stress σ_{eq} and the properties and volume fractions $c^{(r)}$ of the individual phases. The compliance θ^{hom} is determined by using the homogenization technique developed recently by Ponte Castañeda, Suquet and co-workers [7, 9, 10] for non-linear composites. Each of the individual phases (r) is assumed to obey a viscoplastic equation of the form

$$\begin{aligned} \mathbf{D}^{p(r)} &= \frac{1}{2} \theta^{(r)} \mathbf{s}^{(r)} = \dot{\epsilon}^{p(r)} \mathbf{N}^{(r)}, \quad \dot{\epsilon}^{p(r)} = \frac{1}{3} \sigma_{eq}^{(r)} \theta^{(r)}, \\ \dot{\epsilon}^{p(r)} &= \dot{\epsilon}_o^{(r)} \left[\frac{\sigma_{eq}^{(r)}}{\sigma_y^{(r)} (\bar{\epsilon}^{p(r)})} \right]^{m^{(r)}} \end{aligned} \quad (8)$$

where $\dot{\epsilon}_o^{(r)}$ and $m^{(r)}$ are constants and $\sigma_y^{(r)}$ is the yield stress of phase (r) that depends on the corresponding equivalent plastic strain $\bar{\epsilon}^{p(r)}$. It should be noted that in the limit as $m^{(r)} \rightarrow \infty$, the above equations reduce to a rate-independent von Mises plasticity model with flow $\sigma_y^{(r)}$.

A brief description of the methodology that determines θ^{hom} , for given values $(\sigma_{eq}, c^{(r)}, \bar{\epsilon}^{p(r)})$, is given in the following. Consider a linear composite with (as yet unknown) compliances $\theta^{(r)}$, $r = 1, 2, 3, 4$, and a linear theory that provides an expression for the θ^{hom} in terms of the aforementioned $\theta^{(r)}$. In our case, the following Hashin-Shtrikman estimate is used

$$\frac{1}{\theta^{\text{hom}}} = \left(\sum_{r=1}^4 \frac{c^{(r)}}{\frac{1}{\theta^{(r)}} + \frac{3}{2\theta^{(0)}}} \right) / \left(\sum_{r=1}^4 \frac{c^{(r)}}{\frac{1}{\theta^{(r)}} + \frac{3}{2\theta^{(0)}}} \right) \quad (9)$$

with $\theta^{(0)} = \theta^{(4)}$ the compliance of the ferritic matrix phase (4). Then, the following eight non-linear equations ($r = 1, 2, 3, 4$) (Suquet [9, 10])

$$\theta^{(r)} = \frac{3 \dot{\varepsilon}^{p(r)}}{\sigma_{eq}^{(r)}} = \frac{3 \dot{\varepsilon}_o^{(r)}}{\sigma_{eq}^{(r)}} \left[\frac{\sigma_{eq}^{(r)}}{\sigma_y^{(r)} (\bar{\varepsilon}^{p(r)})} \right]^{m^{(r)}}$$

and

$$\sigma_{eq}^{(r)} = \sigma_{eq} \sqrt{\frac{1}{c^{(r)}} \frac{\partial \theta^{hom}}{\partial \theta^{(r)}}}$$

are solved for $(\theta^{(r)}, \sigma_{eq}^{(r)})$. Finally θ^{hom} is determined from (9). In the process of the solution, the average strain rate $\dot{\varepsilon}^{p(r)}$ in the phases are determined as well. The above methodology is a special case of the so-called “modified secant method” [9, 10] which coincides with the variational procedure of Ponte Castañeda [7].

Phase Hardening. The individual constituents of the composite material exhibit different hardening behaviour during the deformation process. The selected hardening curves accounting for the hardening behaviour of the four phases are presented in **figure 1**. The hardening behaviour of martensite is obtained from experimental data of a partly martensitic steel (volume fraction of martensite $\cong 95\%$) presented in [1]. Input data for the hardening behaviour of the ferritic phase is obtained from experimental results for an annealed steel also presented in [1]. The hardening behaviour of bainite is obtained from tensile tests performed in a 0.5% C steel subjected to thermal treatment in the range of bainite formation and presented in [1]. The hardening curve for the austenite is obtained from experimental data given in [3]. It should be mentioned that the behaviour of martensite does not vary substantially with temperature in the range considered in figure 1.

Transformation kinetics model. The evolution of martensite due to martensitic transformation is described by a transformation kinetics model which takes into account temperature, plastic strain, and stress state. This kinetic model was first proposed by Olson and Cohen [4] and then modified in a generalized rate form by Stringfellow et al. [8], so as to incorporate pressure sensitivity into the model. The model of Olson and Cohen assumes that the rate of increase of the volume fraction of martensite \dot{f} is proportion-

al to the rate of increase of the number of martensitic embryos per unit austenite volume and is based on the experimental observation that strain-induced nucleation of martensite occurs predominantly at shear band intersections within austenite. The kinetic model used in the present work is a generalization of what was proposed by Stringfellow et al. [8] for two-phase steels in the form

$$\dot{f} = c^{(a)} \left(A_f \dot{\varepsilon}^{p(a)} + B_f \dot{\Sigma} \right) \quad (10)$$

where $\dot{\varepsilon}^{p(a)} = \dot{\varepsilon}^{p(2)}$ is the rate of the equivalent plastic strain in austenite and the factor $c^{(a)} = c^{(2)}$ reflects the decreasing volume fraction of austenite available for transformation. The parameter Σ is a measure of the “triaxiality” of the stress state and is defined as

$$\Sigma = \frac{p}{\sigma_{eq}} \quad (11)$$

where $p = \sigma_{kk}/3$ is the ratio of the hydrostatic stress. The coefficients A_f and B_f are functions of stress state, plastic strain and the volume fraction of martensite for constant temperature. The coefficient A_f is determined from (Stringfellow et al. [8])

$$A_f = \alpha \beta_0 r (1 - f_{sb}) (f_{sb})^{r-1} P \quad (12)$$

where α represents the rate of shear band formation and is a function of temperature, the exponent r models the orientation of shear bands and β_0 is a function of temperature. The parameter f_{sb} represents the volume fraction of shear bands and depends on plastic strain in the austenite, as follows:

$$f_{sb} = 1 - e^{-\alpha \bar{\varepsilon}^{p(a)}} \quad (13)$$

The number of operational nucleation sites is assumed to equal the number of shear band intersections per unit volume multiplied by the probability P that a shear band intersection will act as a nucleation site. The probability P is determined from (Stringfellow et al. [8])

$$P(g) = \frac{1}{\sqrt{2\pi} s_g} \int_{-\infty}^g \exp \left[-\frac{1}{2} \left(\frac{g - \bar{g}}{s_g} \right)^2 \right] dg \quad (14)$$

where \bar{g} and s_g are the dimensionless mean and the standard deviation of the probability distribution function. The probability P is a function of temperature and stress state through the argument of the distribution function g . The parameter g is a normalized net thermodynamic driving force defined as

$$g = g_0 - g_1 \Theta + g_2 \Sigma \quad (15)$$

where g_0, g_1 and g_2 are dimensionless constants and Θ is a normalized temperature which is related to the absolute temperature T according to

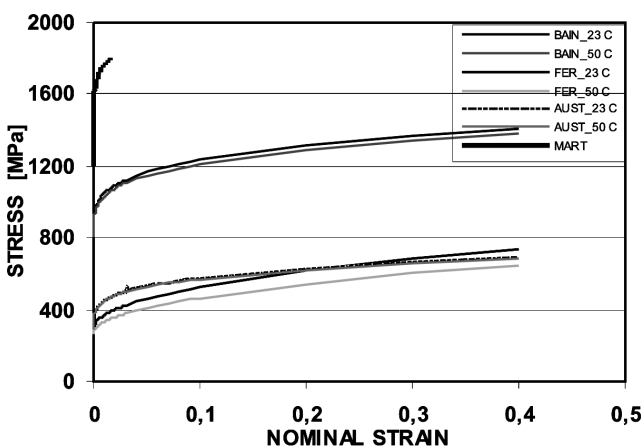


Figure 1: Hardening behaviour of individual phases.

$$\Theta = \frac{T - M_{s,ut}^\sigma}{M_{d,ut} - M_{s,ut}^\sigma} \quad (16)$$

where $M_{d,ut}$, $M_{s,ut}^\sigma$ are the M_d and M_s^σ temperatures for uni-axial tension, M_d is the temperature below which no transformation is observed, and M_s^σ the temperature above which the transformation stress exceeds that of the parent phase such that transformation is preceded by significant plastic yielding. The parameter B_f is determined as follows (Stringfellow *et al.* [8])

$$B_f = 0 \text{ if } \Delta\Sigma \leq 0, \text{ and}$$

$$B_f = \frac{g_2}{\sqrt{2\pi} s_g} \beta_0 (f_{sb})^r \exp\left[-\frac{1}{2} \left(\frac{g - \bar{g}}{s_g}\right)^2\right] \text{ if } \Delta\Sigma > 0.$$

Summary of constitutive equations. The final form of the constitutive model that describes the mechanical behaviour of multiphase TRIP steels is as follows:

$$\mathbf{D} = \mathbf{D}^e + \mathbf{D}^p + \mathbf{D}^{TRIP} \quad (17)$$

$$\mathbf{D}^e = \mathbf{M}^e : \overset{\nabla}{\boldsymbol{\sigma}} \Leftrightarrow \overset{\nabla}{\boldsymbol{\sigma}} = \mathbf{L}^e : \mathbf{D}^e \quad (18)$$

$$\mathbf{D}^p = \dot{\boldsymbol{\varepsilon}}^p \mathbf{N}, \quad \dot{\boldsymbol{\varepsilon}}^p = \frac{1}{3} \sigma_{eq} \theta^{\text{hom}}, \quad \mathbf{N} = \frac{3}{2} \frac{\mathbf{s}}{\sigma_{eq}} \quad (19)$$

$$\mathbf{D}^{TRIP} = \left[A (\sigma_{eq}) \mathbf{N} + \frac{\Delta_v}{3} \boldsymbol{\delta} \right] \dot{f} \quad (20)$$

$$\dot{f} = c^{(a)} \left(A_f \dot{\boldsymbol{\varepsilon}}^{p(a)} + B_f \dot{\Sigma} \right) \quad (21)$$

$$\dot{c}^{(a)} = - \left[1 - (c^{(3)} + c^{(4)}) \Delta_v \right] \dot{f} \quad (22)$$

$$\dot{c}^{(3)} = -c^{(3)} \Delta_v \dot{f}, \quad \dot{c}^{(4)} = -c^{(4)} \Delta_v \dot{f}. \quad (23)$$

Numerical integration and finite element implementation of the constitutive model

In a finite element environment, the solution is developed incrementally and the constitutive equations are integrated numerically at the element Gauss points. In a displacement based finite element formulation the solution is deformation driven. Let \mathbf{F} denote the deformation gradient tensor. At a given Gauss point, the solution $(\mathbf{F}_n, \boldsymbol{\sigma}_n, c_n^{(r)})$ at time t_n as well as the deformation gradient \mathbf{F}_{n+1} at time $t_{n+1} = t_n + \Delta t$ are known and the problem is to determine $(\boldsymbol{\sigma}_{n+1}, c_{n+1}^{(r)})$. The time variation of the deformation gradient \mathbf{F} during the time increment $[t_n, t_{n+1}]$ can be written as

$$\mathbf{F}(t) = \Delta\mathbf{F}(t) \cdot \mathbf{F}_n = \mathbf{R}(t) \cdot \mathbf{U}(t) \cdot \mathbf{F}_n, \quad t_n \leq t \leq t_{n+1}$$

where $\mathbf{R}(t)$ and $\mathbf{U}(t)$ are the rotation and right stretch tensors associated with $\Delta\mathbf{F}(t)$. The corresponding deformation rate $\mathbf{D}(t)$ tensor can be written as:

$$\mathbf{D}(t) = [\dot{\mathbf{F}}(t) \cdot \mathbf{F}^{-1}(t)]_s = [\Delta\dot{\mathbf{F}}(t) \cdot \Delta\mathbf{F}^{-1}(t)]_s$$

where the subscripts s and a denote the symmetric and anti-symmetric parts respectively of a tensor. If it is assumed that the Lagrangian triad associated with $\Delta\mathbf{F}(t)$ (i.e., the eigenvectors of $\mathbf{U}(t)$) remains fixed in the time period $[t_n, t_{n+1}]$, then it can readily be shown that

$$\begin{aligned} \mathbf{D}(t) &= \mathbf{R}(t) \cdot \dot{\mathbf{E}}(t) \cdot \mathbf{R}^T(t), \\ \mathbf{W}(t) &= \dot{\mathbf{R}}(t) \cdot \mathbf{R}^T(t) \cdot \mathbf{R}^T(t) \end{aligned} \quad (24)$$

and

$$\overset{\nabla}{\boldsymbol{\sigma}}(t) = \mathbf{R}(t) \cdot \dot{\boldsymbol{\sigma}}(t) \cdot \mathbf{R}^T(t) \quad (25)$$

where $\mathbf{E}(t) = \ln \mathbf{U}(t)$ is the logarithmic strain associated with the increment, $\dot{\boldsymbol{\sigma}}(t) = \mathbf{R}^T(t) \cdot \boldsymbol{\sigma}(t) \cdot \mathbf{R}(t)$. It is noted that at the start of the increment:

$$\Delta\mathbf{F}_n = \mathbf{R}_n = \mathbf{U}_n = \boldsymbol{\delta}, \quad \dot{\boldsymbol{\sigma}}_n = \boldsymbol{\sigma}_n \quad \text{and} \quad \mathbf{E}_n = \mathbf{0},$$

whereas at the end of the increment:

$$\Delta\mathbf{F}_{n+1} = \mathbf{F}_{n+1} \cdot \mathbf{F}_n^{-1} = \mathbf{R}_{n+1} \cdot \mathbf{U}_{n+1} = \text{known, and}$$

$$\mathbf{E}_{n+1} = \ln \mathbf{U}_{n+1} = \text{known.}$$

Taking into account (24) and (25), we can write the elastoplastic equations in the form

$$\dot{\mathbf{E}} = \dot{\mathbf{E}}^e + \dot{\mathbf{E}}^p + \dot{\mathbf{E}}^{TRIP} \quad (26)$$

$$\dot{\boldsymbol{\sigma}} = \mathbf{L}^e : \dot{\mathbf{E}}^e \quad (27)$$

$$\dot{\mathbf{E}}^p = \dot{\boldsymbol{\varepsilon}}^p \hat{\mathbf{N}},$$

$$\dot{\boldsymbol{\varepsilon}}^p = \frac{1}{3} \sigma_{eq} \theta^{\text{hom}}, \quad \hat{\mathbf{N}} = \frac{3}{2} \frac{\hat{\mathbf{s}}}{\sigma_{eq}} \quad (28)$$

$$\dot{\mathbf{E}}^{TRIP} = \left[A (\sigma_{eq}) \hat{\mathbf{N}} + \frac{\Delta_v}{3} \boldsymbol{\delta} \right] \dot{f} \quad (29)$$

$$\dot{f} = c^{(a)} \left(A_f \dot{\boldsymbol{\varepsilon}}^{p(a)} + B_f \dot{\Sigma} \right) \quad (30)$$

$$\dot{c}^{(a)} = - \left[1 - (c^{(3)} + c^{(4)}) \Delta_v \right] \dot{f} \quad (31)$$

$$\dot{c}^{(3)} = -c^{(3)} \Delta_v \dot{f}, \quad \dot{c}^{(4)} = -c^{(4)} \Delta_v \dot{f}. \quad (32)$$

Integration of equation (26) gives

$$\Delta\mathbf{E} = \Delta\mathbf{E}^e + \Delta\mathbf{E}^p + \Delta\mathbf{E}^{TRIP} \quad \text{or}$$

$$\Delta\mathbf{E}^e = \Delta\mathbf{E} - \Delta\mathbf{E}^p - \Delta\mathbf{E}^{TRIP}. \quad (33)$$

Integration of equation (27) yields $\Delta \hat{\boldsymbol{\sigma}} = \mathbf{L}^e : \Delta \mathbf{E}^e$ or

$$\hat{\boldsymbol{\sigma}}_{n+1} = \hat{\boldsymbol{\sigma}}^e - \mathbf{L}^e : (\Delta \mathbf{E}^p + \Delta \mathbf{E}^{TRIP}) \quad (34)$$

where $\hat{\boldsymbol{\sigma}}^e = \hat{\boldsymbol{\sigma}}_n + \mathbf{L}^e : \Delta \mathbf{E}$ is known is the “elastic predictor”. Equations (28), (29) and (30) are integrated using the backward Euler method

$$\Delta \mathbf{E}^p = \frac{1}{3} \sigma_{eq}|_{n+1} \theta_{n+1}^{hom} \Delta t \hat{\mathbf{N}}_{n+1} \quad (35)$$

$$\Delta \mathbf{E}^{TRIP} = \left[A \left(\sigma_{eq}|_{n+1} \right) \hat{\mathbf{N}}_{n+1} + \frac{\Delta v}{3} \boldsymbol{\delta} \right] \Delta f. \quad (36)$$

$$\Delta f = c_{n+1}^{(a)} \left(A_f|_{n+1} \dot{\varepsilon}_{n+1}^{p(a)} \Delta t + B_f|_{n+1} \Delta \Sigma \right) \quad (37)$$

Equations (32) are integrated exactly:

$$c_{n+1}^{(3)} = c_n^{(3)} e^{-\Delta v \Delta f}, \quad c_{n+1}^{(4)} = c_n^{(4)} e^{-\Delta v \Delta f} \quad (38)$$

and $c_{n+1}^{(a)}$ is determined from

$$c_{n+1}^{(a)} = 1 - f_{n+1} - c_{n+1}^{(3)} - c_{n+1}^{(4)}. \quad (39)$$

Finally, Σ is determined from the equation

$$\Delta \Sigma = \Sigma_{n+1} - \Sigma_n = \left(\frac{p}{\sigma_{eq}} \right)_{n+1} - \left(\frac{p}{\sigma_{eq}} \right)_n. \quad (40)$$

Substituting the above equations into the elasticity equation (34) and evaluating the deviatoric part of $\hat{\boldsymbol{\sigma}}_{n+1}$, we conclude that the deviatoric parts of $\hat{\boldsymbol{\sigma}}_{n+1}$ and $\hat{\boldsymbol{\sigma}}^e$ are collinear. Therefore

$$\hat{\mathbf{N}}_{n+1} = \frac{3}{2} \frac{\hat{\boldsymbol{\sigma}}_{n+1}}{\sigma_{eq}|_{n+1}} = \frac{3}{2} \frac{\hat{\boldsymbol{\sigma}}^e}{\sigma_{eq}^e} = \text{known.}$$

Then, projecting the stress tensor onto the deviatoric plane ($\sigma_{eq} = \hat{\boldsymbol{\sigma}} : \hat{\mathbf{N}} = \boldsymbol{\sigma} : \mathbf{N}$) and the pressure axis ($p = \hat{\boldsymbol{\sigma}} : \boldsymbol{\delta}/3 = \boldsymbol{\sigma} : \boldsymbol{\delta}/3$) we obtain the following equations:

$$\begin{aligned} \sigma_{eq}|_{n+1} &= \sigma_{eq}^e - 3G \Delta \varepsilon_q, \\ p_{n+1} &= p^e - K \Delta v \Delta f \end{aligned} \quad (41)$$

where σ_{eq}^e and p^e are the elastic shear and bulk modulus respectively, $\sigma_{eq}^e = \hat{\boldsymbol{\sigma}}^e : \hat{\mathbf{N}} = \sqrt{3 s_{ij}^e s_{ij}^e}$ is the equivalent stress of the elastic $\hat{\boldsymbol{\sigma}}^e$, and

$$\Delta \varepsilon_q = \frac{1}{3} \sigma_{eq}|_{n+1} \theta_{n+1}^{hom} \Delta t + A \left(\sigma_{eq}|_{n+1} \right) \Delta f. \quad (42)$$

The integration algorithm can be summarized as follows. The quantities Δf and $\Delta \varepsilon_q$ are chosen as the primary unknowns and equations (37) and (42) are treated as the basic equations in which $\sigma_{eq}|_{n+1}, p_{n+1}, \Delta \Sigma, c_{n+1}^{(a)}, c_{n+1}^{(3)}$ and $c_{n+1}^{(4)}$

are defined by equations (41), (40), (39) and (38). Equations (37) and (42) are solved for Δf and $\Delta \varepsilon_q$ by using Newton’s method. Once Δf and $\Delta \varepsilon_q$ are found, equations (41), (38), (39) and (40) define $\sigma_{eq}|_{n+1}, p_{n+1}, \Delta \Sigma, c_{n+1}^{(3)}, c_{n+1}^{(4)}$ and $c_{n+1}^{(a)}$. Then $\hat{\boldsymbol{\sigma}}_{n+1}$ is determined from

$$\hat{\boldsymbol{\sigma}}_{n+1} = \frac{2}{3} \sigma_{eq}|_{n+1} \hat{\mathbf{N}}_{n+1} + p_{n+1} \boldsymbol{\delta}. \quad (43)$$

Finally, $\boldsymbol{\sigma}_{n+1}$ is computed from

$$\boldsymbol{\sigma}_{n+1} = \mathbf{R}_{n+1} \cdot \hat{\boldsymbol{\sigma}}_{n+1} \cdot \mathbf{R}_{n+1}^T \quad (44)$$

which completes the integration process.

The corresponding “linearization moduli” of the algorithm have been presented by Papatriantafillou in [6].

Results

The constitutive model presented in the previous sections is implemented in the ABAQUS general-purpose finite element program. This code provides a general interface so that a particular constitutive model can be introduced as a “user subroutine”.

The values $E = 200$ GPa and $\nu = 0.3$ for the elastic Young’s modulus and Poisson’s ratio are used in the calculations. The curves that define the variation of the flow stress of the phases $\sigma_y^{(r)}$ ($\bar{\varepsilon}^{p(r)}$) are shown in **figure 1**. The values $\dot{\varepsilon}_0^{(r)} = 10^{-4} \text{sec}^{-1}$ and $m^{(r)} = 60$ are used for all four phases. The large value of the strain-rate exponent $m^{(r)}$ makes the behaviour of the phases essentially rate-independent. The relative volume change associated with the martensitic transformation takes the value $\Delta v = 0.02$. Experimental data for uniaxial tension of a TRIP steel in two temperatures (room temperature and 50°C) are used for the calibration of the model. This leads to the values $A_0 = 0.012, A_1 = 0.057, s_a^* = 496$ MPa, $g_0 = 3400, g_1 = 4.7, g_2 = 493, \bar{g} = 3230, s_g = 292, M_{d,ut} = 52^\circ\text{C}, M_{s,ut} = 10^\circ\text{C}$ and $r = 2$. The variation of α and β_0 with temperature is given in **table 1**.

The amount of retained austenite experimentally observed before straining is 12% while the volume fractions of ferrite and bainite are 50% and 38% respectively, i.e., the initial volume fractions are $f_0 = 0, c_0^{(a)} = 0.12, c_0^{(3)} = 0.38$ and $c_0^{(4)} = 0.50$. Experiments show that, in uniaxial tension, some amount of martensite appears before yielding takes place; this is due to “stress induced” transformation. In order to account for this effect, since our model considers plastic-strain-induced transformation only, we modify the initial values of f and to $f_0 = 0.017, c_0^{(a)} = 0.103$ at room temperature, and $f_0 = 0.013, c_0^{(a)} = 0.107$ at 50°C.

Figures 2 and 3 show the predicted σ – ε and f – ε curves in uniaxial tension together with the experimental data at room temperature and at 50°C. The predictions of the model are obtained by using one isoparametric axisymmetric finite element loaded in uniaxial tension; 2X2 Gauss integration stations and the so-called B-bar method are used in the computations. The higher amount of martensite formed at room temperature is responsible for the higher level of hardening observed in the same temperature.

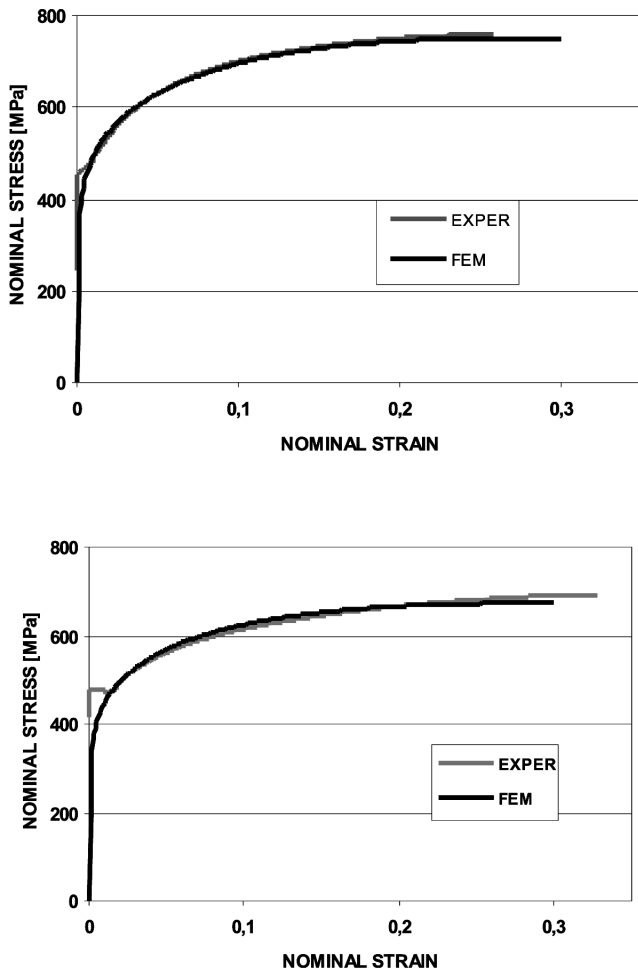


Figure 2: Stress-strain curves in uniaxial tension at room temperature (above) and at 50°C (below). Experimental results and model predictions.

The model is used also for the simulation of necking in a uniaxial tension test using the finite element method. A cylindrical specimen is analyzed with aspect ratio $L_0/R_0 = 3$, where $2L_0$ is the initial length of the specimen and R_0 its initial radius. Because of symmetry, only one half of the cylindrical specimen is analysed. The deformation is driven by the uniform prescribed end displacement in the axial direction on the shear free end while the lateral surface of the specimen is kept traction free. The finite elements used in the computations are the same as that used in the problem of uniaxial tension. In order to promote necking, a geometric imperfection is introduced. In particular, the undeformed configuration of the specimen is perturbed in a way resembling the necking mode, i.e., the initial radius R of the specimen is assumed to vary in the axial z -direction according to the formula

$$R(z) = R_0 - \xi R_0 \cos \frac{\pi z}{2 L_0}$$

where the $\xi = 0.005$ is used, and the plane $z = 0$ coincides with the middle cross section of the specimen.

Figure 4 shows the σ - ε curves for both a transforming and a non-transforming material at room temperature. The

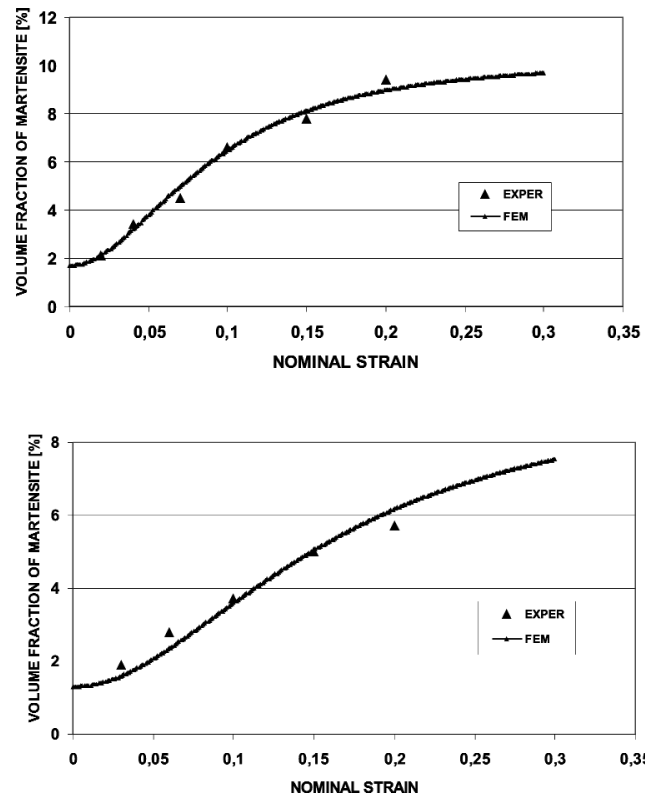


Figure 3: volume fraction of martensite f in uniaxial tension at room temperature (above) and at 50°C (below). Experimental results and model predictions.

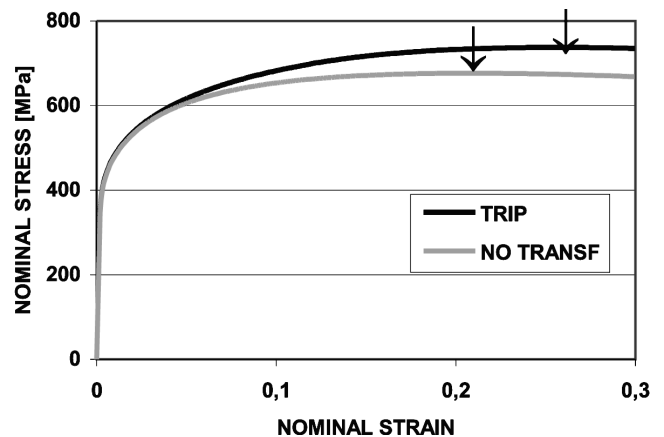


Figure 4: Stress-strain curves in uniaxial tension with and without TRIP.

Table 1: Values used in the kinetics model

T	α	β_0
23 °C	8.7	1.8
50 °C	5.2	1.5

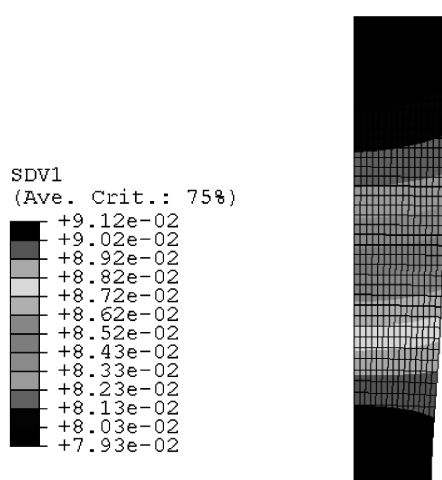
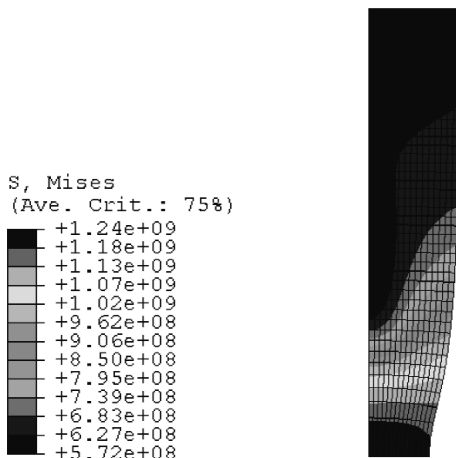
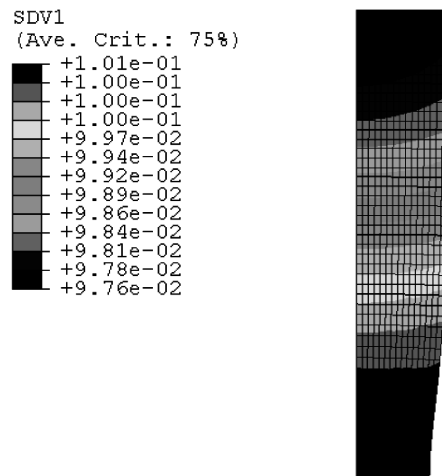
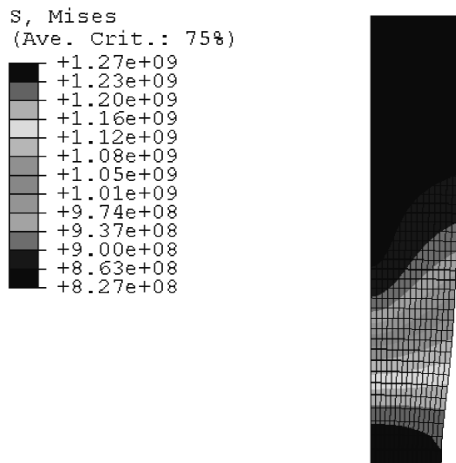


Figure 5: Contours of von Mises equivalent stress (in Pa) with and without transformation at a nominal strain level of 50%.

Figure 6: Contours of volume fraction of martensite f at room temperature (above) and at 50°C (below) at a nominal strain of 50%.

two arrows on the curves indicate the point of maximum load, which coincides with end of uniform elongation of the specimen; it is clear that TRIP increases substantially the range of stable deformation. **Figure 5** shows contours of the von Mises equivalent stress σ_{eq} (in Pa) with and without transformation at a nominal strain level of 50%. Formation of martensite leads to stabilization of necking, and propagation of the neck down the length of the specimen. **Figure 6** shows contours of f for the transforming material at a nominal strain of 50% at room temperature and at 50°C. The TRIP effect is more pronounced at room temperature as expected.

Acknowledgement

This work has been partially supported by the European Commission through the projects ECSC 7210-PR-161 and ECSC 7210-PR-370.

(A2004085)

Contact: Professor Dr. Ing. Nikolaos Aravas
 Department of Mechanical and Industrial Engineering
 University of Thessaly, Volos, Greece

References

- [1] Final report of technical steel research with title: Modelling of mechanical properties and local deformation of high-strength multi-phase steels, European Commission, Contract No 7210-PR/044.
- [2] H.G. Hopkins and M.J. Sewell: Elasticity Theory of Composites, Mechanics of Solids, The Rodney Hill 60th Anniversary Volume, Pergamon Press, (1980), pp. 653-686.
- [3] T. Naturani, G.B. Olson, M. Cohen: Journal de Physique, 43 (1982), 429-434.
- [4] G.B. Olson, M. Cohen: Metallurgical Transactions A, 7A (1976), 1897-1923.
- [5] G.B. Olson, T. Tsuzaki, M. Cohen: Statistical Aspects of Martensitic Nucleation, Mater. Res. Soc. Symp. Proc., 1987, Vol. 57, pp. 129-148.
- [6] I. Papatriantafyllou, "TRIP steels: Constitutive modelling and computational issues", Ph.D. thesis, Dept. of Mechanical and Industrial Engng, University of Thessaly, Greece (2004).
- [7] P. Ponte Castañeda, P. Suquet: Nonlinear composites, Advances in Applied Mechanics, Academic Press, (1998), Vol. 34, pp. 171-302.
- [8] R.G. Stringfellow, D.M. Parks, G.B. Olson: Acta Metall., 40 (1992), 1703-1716.
- [9] P. Suquet: C. R. Acad. Sc. Paris, Iib, 320 (1995) pp. 563-571.
- [10] P. Suquet: Overall properties of nonlinear composites, IUTAM Symposium on Micromechanics of Plasticity and damage of Multi-phase Materials, Kluwer Academic Publishers, (1996), pp. 149-156.